INTERNATIONAL ATOMIC ENERGY AGENCY
UNITED NATIONS EDUCATIONAL, SCIENTIFIC AND CULTURAL ORGANIZATION
INTERNATIONAL CENTRE FOR THEORETICAL PHYSICS
I.C.T.P., P.O. BOX 586, 34100 TRIESTE, ITALY, CABLE: CENTRATOM TRIESTE

SMR/697
5-Mag. Mult.

RESEARCH WORKSHOP ON CONDENSED MATTER PHYSICS
(21 June - 3 September 1993)

WORKING GROUP ON MAGNETIC MULTILAYERS
(9 - 13 August 1993)

INTINERANT MAGNETISM OF DISORDERED Fe-Co and Ni-Cu ALLOYS IN TWO AND THREE DIMENSIONS

J. KUNDROVSKY
Institute of Physics
Czech. Academy Sci.
CZ-18040 Praha
CZECH REPUBLIC

Itinerant magnetism of disordered Fe-Co and Ni-Cu alloys in two and three dimensions

I. Turek [a], J. Kudrnovský [b,c], V. Drchal [b], and P. Weinberger [c]

[a] *Institute of Physical Metallurgy, Czech Academy of Sciences, CZ-616 62 Brno, Czech Republic*

[b] *Institute of Physics, Czech Academy of Sciences, CZ-180 40 Praha 8, Czech Republic*

[c] *Institute for Technical Electrochemistry, Technical University, A-1060 Vienna, Austria*

Abstract

The electronic structure and band magnetism of disordered bcc $Fe_{100-x}Co_x$ and fcc $Ni_{100-x}Cu_x$ bulk alloys and their disordered epitaxial overlayers on an fcc Cu(001) substrate were studied by means of first-principles tight binding linear muffin-tin orbital method combined with the coherent potential approximation. For the Fe-Co system, we have found that the composition dependence of the averaged and local Fe magnetic moments is strongly affected by the dimensionality of the system while the local Co moments remain nearly constant. In the bulk bcc alloys, a non-monotonous behavior of the averaged magnetization occurs due to the transition from weak to strong ferromagnetism. The averaged magnetization of the random overlayers depends linearly on the composition while the local Fe and Co moments are constant since the strong ferromagnetism is stabilized by the substrate throughout the whole composition range. For the Ni-Cu system, a transition from ferromagnetism to paramagnetism is found both in the bulk fcc alloys and in the overlayers. The ferromagnetism of the overlayers is reduced in comparison to the bulk systems of the same composition. Further electronic characteristics (local densities of states, local numbers of electrons, and work functions) are presented for both systems and their concentration trends are discussed.

73.20.At, 75.10.Lp, 75.30.Cr, 75.70.Ak

I. INTRODUCTION

Recent investigations of two-dimensional magnetism of metallic surfaces, interfaces and ultrathin films [1] have become possible due to modern techniques of sample preparation and characterization [2] as well as due to the progress in first-principles electronic structure calculations [3]. The unexpected magnetic properties of these systems, which offer promising technological applications, are to a large extent due to their chemically perfect layered structures. This fact has motivated systematic ab-initio studies of electronic and magnetic properties of metallic systems with ideal interfaces aiming both at deeper understanding of these properties and at quantitative predictions for realistic systems [3].

The magnetic properties of systems with chemical or topological disorder can be even more interesting. The random binary bcc Fe-Co and fcc Ni-Cu alloys represent only two examples proving how much the present knowledge of bulk itinerant magnetism benefited from detailed studies of alloys containing transition 3d-metals. In the bcc Fe-Co alloys, which can be prepared up to 70 at % Co, the saturation magnetization depends non-monotonously on the composition, reaching a maximum at about 30 at % Co [4]. This dependence is essentially insensitive to the degree of chemical short-range order and was successfully reproduced by first principles electronic structure calculations based on the local-spin-density approximation (LSDA) for the ordered structures [5] as well as for the disordered alloys [6,7]. The key factors determining the magnetic behavior of this system are the greater electronegativity of Co and the greater exchange splitting of Fe [5–8]. As a consequence, the majority (spin-up) electrons see nearly no difference between the alloy constituents, in contrast to the minority (spin-down) electrons which feel a stronger disorder in the atomic 3d levels. This leads to a transition from the weak itinerant ferromagnetism of the Fe-rich alloys to the strong ferromagnetism of the Co-rich alloys.

While the effect of the Fe-Co alloying on magnetism is well explored in the bulk, this problem has not been addressed in two dimensions yet. Recent progress in preparation techniques has lead to ultrathin transition-metal films (down to 1 monolayer) deposited

on noble-metal substrates, e.g. Co/Cu(001). Owing to the easy Fe-Co solubility together with the negligible Fe-Cu and Co-Cu solubilities, random Fe-Co monolayers on the Cu(001) substrate can serve as possible realistic models of two-dimensional itinerant ferromagnetism of binary alloys. Their electronic and magnetic properties can be then investigated similarly as for pure Fe and Co monolayers on the Cu(001) substrate [3,9].

The Ni-Cu alloy exhibits behavior substantially different from the Fe-Co system. In the bulk, a transition from Ni-rich ferromagnetic systems to Cu rich alloys without local magnetic moments was found experimentally at approximately 55 at % Cu together with the fact that the local magnetic moments of Cu atoms are negligible at all compositions [10]. Theoretical reasons for the observed composition dependence of the Ni moments were given for artificial ordered fcc-based structures [11] as well as for fcc disordered alloys [7]. The main conclusion of these studies is the rejection of the rigid-band model for this system, in spite of the simple composition dependence of the averaged magnetization. In the Ni/Cu layered structures, the mutual interdiffusion of both constituents can be hardly avoided [2]. The realistic models of Ni thin films on Cu substrates should take this phenomenon and its influence on electronic and magnetic properties into account. A recent ab initio study of this type was performed for Ni films sandwiched by two semiinfinite Cu(111) crystals with different degrees of interdiffusion [12]. For the Ni films on the Cu surface, only chemically perfect one and two Ni monolayers on the Cu(001) face have been investigated so far [13].

The purpose of this paper is a first-principles investigation of the electronic structure and itinerant magnetism of disordered $Fe_{100-x}Co_x$ and $Ni_{100-x}Cu_x$ alloys in the bulk and as two-dimensional monolayers on the Cu(001) substrate. We employ the tight binding linear muffin-tin orbital method (TB-LMTO) in the atomic sphere approximation (ASA) [14] combined with the coherent potential approximation (CPA) to describe the chemical disorder in the bulk [15] and in the overlayer [16]. The formalism used in this paper is similar to that developed in Ref. [17] for the case of clean magnetic surfaces. The method is briefly described in the next section, the results are presented and discussed in the Section 3.

II. FORMALISM AND COMPUTATIONAL DETAILS

Our description of the bulk and surface electronic structure in the presence of chemical disorder is based on the TB LMTO ASA second-order Hamiltonian H [14] and the corresponding Green's functions $G(z) = (z - H)^{-1}$ and $g(z) = (P(z) - S)^{-1}$ [15,16]. Here the quantities $G(z)$, H, $g(z)$, $P(z)$ and S are matrices with indices $RL, R'L'$ where R, R' are site indices and L, L' are orbital indices. The matrix $P(z)$ is a diagonal matrix of screened potential functions $P_{RL}(z)$ parametrized by means of three potential parameters [14] which describe the scattering properties of the individual atomic spheres. The matrix S is a non-diagonal matrix of screened structure constants $S_{RL,R'L'}$ which contain the information on the geometry of the system. The Green's functions $G(z)$ and $g(z)$ are related by a simple scaling transformation [15], the former being directly connected with physical quantities, the latter being indispensable for systems with perturbed translational symmetry.

In the presence of substitutional chemical disorder, the potential functions $P_{RL}(z)$ of some sites R take randomly two values $P^A_{RL}(z)$ and $P^B_{RL}(z)$ with probabilities c^A_R and c^B_R (concentrations of the chemical elements A and B), respectively. The configurational average of the Green's function $g(z)$ in the single site CPA can be expressed as

$$g(z) = \langle (P(z) - S)^{-1} \rangle = (\mathcal{P}(z) - S)^{-1} , \tag{1}$$

Here the quantity $\mathcal{P}(z)$ is a site diagonal matrix of the so-called coherent potential functions $\mathcal{P}_{RL}(z)$. The coherent potential functions are equal to the original potential functions for sites without disorder. For a site R with disorder, the corresponding coherent potential function fulfils the CPA selfconsistency condition

$$\sum_{AB} c^A_R t^{AB}_R(z) = 0 , \tag{2}$$

$$t^{AB}_R(z) = [P^{AB}_R(z) - \mathcal{P}_R(z)]\{1 + \Phi_R(z)[P^{AB}_R(z) - \mathcal{P}_R(z)]\}^{-1} ,$$

where the quantities $t_R(z)$, $P_R(z)$, $\mathcal{P}_R(z)$, $\Phi_R(z)$ are matrices in the orbital indices L, L'. The quantity $t^{AB}_R(z)$ represents the single site t matrix and the quantity $\Phi_R(z) = g_{RR}(z)$ is

the site-diagonal block of the averaged Green's function matrix $g(z)$. According to Eq. (1), this quantity is determined by the non-random coherent potential function $\mathcal{P}(z)$ and by the geometry of the system. This means that the full symmetry of the averaged system can be used to evaluate all elements of $g(z)$.

The calculation of $g(z)$ for bulk cubic alloys is thus performed by standard Brillouin zone (BZ) integration techniques [15]. In the case of surfaces, one must employ the underlying two-dimensional translational symmetry in the directions parallel to the surface and handle the semiinfinite nature in the perpendicular direction [16,18,19]. We use an efficient technique based on the short ranged screened structure constants S and on the surface Green's functions (SGF) [16,18]. The short range character of S allows to conceive the system as a stacking of the so-called principal layers (PL) parallel to the surface. These PLs are introduced in such a way that only nearest-neighbour PLs are connected by the structure constants S. In our case of the fcc(001) face and with the screened structure constants of the fcc lattice non-zero only up to the nearest neighbours, one PL is equivalent to one atomic (001) layer. The whole system can be then decomposed into three parts: (i) semiinfinite bulk metal with potential parameters identical to those of infinite metal, (ii) semiinfinite vacuum region represented by empty spheres and their potential parameters, and (iii) the intermediate region containing several layers with non-trivial changes of electronic properties. With the above decomposition, the elements of $g(z)$ for sites in the intermediate region can be found by inversion of finite matrices and subsequent integration over the two dimensional surface Brillouin zone (SBZ). The essential point here is the inclusion of both semiinfinite regions via their corresponding SGFs, see Ref. [16] for details.

To achieve the LSDA selfconsistency, the on site elements of the conditionally averaged Green's function $G(z)$ are necessary for the evaluation of charge and spin densities. These on-site blocks are easily obtained from the corresponding on site quantities $\Phi_R(z)$ [15,16]. Their elements diagonal in the orbital index L are sufficient to calculate the spherical part of the charge density within each atomic sphere, while the elements off diagonal in L, L' are also required for the non-spheridized charge densities. Although we performed our

calculation in the ASA, in the overlayer case we have included these non-spherical charges in the intermediate region into the multipole expansions defining interatomic contributions to the Madelung term of the one electron LSDA potentials [16,19,20]. We included monopoles and dipoles for the Madelung terms and for the potential barrier across the surface which leads to satisfactory agreement of the resulting work functions with experiment as well as with full-potential methods.

The formalism described above has been so far applied to non-magnetic systems: random alloys [15], disordered overlayers on pure metallic substrates [16] and surfaces of random alloys [20]. In the present application to the disordered ferromagnetic Fe-Co and Ni-Cu systems, the effect of spin-polarization was included in a way corresponding to the magnetic ground state with collinear spin structure. In this case, all energy dependent quantities appearing in Eqs. (1, 2) acquire also the dependence on the spin index σ ($\sigma = \uparrow, \downarrow$). The CPA part of the problem is then solved for each spin orientation σ separately; the spin-up and spin down parts are mixed in the LSDA step due to the exchange-correlation (XC) part of the density functional. For more details, see Ref. [21].

Our present calculations are non-relativistic, since the relativistic effects are supposed to have negligible influence on the electronic structure and spin magnetic moments of 3d transition metals. We have used the sp^3d^5 LMTO basis for the valence electrons. The core orbitals were recalculated in each LSDA iteration. The energy integrals needed in the LSDA iterations were performed in the complex energy plane over the semi-circle contour starting at a real energy below the bottom of the valence band and ending at the Fermi level. The Fermi level is fixed by the substrate in the overlayer case, but was updated in each iteration in the bulk case. The Green's functions and related energy-dependent quantities needed for the densities of states were calculated in the complex energy plane along a line parallel to the real energy axis with $Im(z) = 0.01$ Ry. The values at the real energies were then obtained by an analytical continuation technique [22].

The bulk systems were treated with the von Barth-Hedin XC potential [23] as parametrized by Moruzzi, Janak and Williams [21] and with the Vosko-Wilk-Nusair XC

potential [25]. The resulting local magnetic moments coincided to 0.02 μ_B, in agreement with previous results [26]. For the BZ integrations, we used 168 and 280 k-points in the irreducible wedge of the bcc and fcc BZ, respectively. In our calculations we benefited from the possibility to have different radii of the atomic spheres for different components [15]. We have kept the ASA radii for both components fixed, corresponding to experimental atomic volumes of the pure metals. The lattice constants and the mean atomic volumes were then calculated according to the Vegard's law. This represents a natural framework for alloys of similar elements where no significant deviations from the Vegard's law can be expected and leads simultaneously to a negligible charge transfer between the alloy constituents.

For the calculation of the disordered overlayers, the intermediate region consisted of five atomic layers: two substrate Cu layers, the disordered overlayer and two layers of empty spheres for a proper treatment of electrons spilt out of the surface. We placed all atoms (and empty spheres) into the positions of the ideal Cu fcc lattice with the experimental lattice constant. We expect that inclusion of the relaxation of the interlayer distances will have no strong influence on the magnetic moments, similarly as for the bcc Fe(001) surface [3]. The LSDA selfconsistency was obtained with the Vosko-Wilk-Nusair XC potential and the irreducible part (1/8) of the fcc(001) SBZ was sampled with 21 special $\mathbf{k}_{\parallel}$ points.

The condition of the charge neutrality cannot be generally fulfilled with only a finite number of layers in the intermediate region. This problem can be solved by a suitable choice of reference levels for the electrostatic potential on both sides of intermediate region [20]. In all studied cases the charge neutrality in the intermediate region was preserved with accuracy of order 0.001 electron.

III. RESULTS

A. Bulk bcc Fe-Co

The calculated compositional dependences of the averaged and local magnetic moments for the bcc $Fe_{100-x}Co_x$ are presented in Fig. 1. We see a non-monotonous dependence of the averaged magnetization $M(x)$ with the maximum near $x \approx 20\%$ which is in good agreement with experiment [4]. The dependence of the Fe moment with increasing Co content is fast increasing up to $x \approx 30\%$ followed by a saturation at higher x at the value $M_{Fe} = 2.6\ \mu_B$. The Co moment holds a constant value of $M_{Co} = 1.7\ \mu_B$ throughout the whole range. Very similar trends were obtained in previous studies [5–7] and seem to be insensitive to details of calculation.

The inspection of the densities of states (DOS) (see Fig. 2 for $Fe_{50}Co_{50}$) and of the local numbers of electrons for both spin orientations (Fig. 3) reveals that the transition from the weak to the strong ferromagnetism occurs at $x \approx 40\%$. This transition is also responsible for the change of the slope of $M(x)$ and $M_{Fe}(x)$. At the Co-rich end, the spin-up DOS is fully occupied and the local numbers of spin up electrons remain constant. The local numbers of spin-down electrons as well as the local magnetic moments are then constant due to the local charge neutrality (see below). At the Fe rich end, the Fermi energy lies in the deep minimum between the bonding and antibonding part of the d-band for the spin-down direction while the spin up DOS is unfilled with approximately 0.3 holes. The Co addition then causes the filling of the spin up band and increases the average and local magnetic moments. The effect is more pronounced for Fe sites with more up-spin holes than for Co sites and is even compensated by appropriate decrease in the local numbers of spin-down electrons (see Fig. 3). These changes in the local numbers of electrons can be conceived as an effective intratomic charge transfer from d↓ to d↑ electrons of Fe atoms which is caused by the Co addition [6,7].

The analysis of the local DOS's (Fig. 2) has confirmed the well known dependence of

the disorder on the spin direction [5–8]. This statement can be put on a more quantitative basis using the selfconsistent potential parameters of the LMTO method [14]. One can identify the potential parameters C (for the d-orbitals) with the "atomic levels" of the alloy components and define the level disorder for both spins as $\delta^\sigma = C^\sigma_{Fe} - C^\sigma_{Co}$. The level disorder for the down-electrons is then $\delta^\downarrow \approx 0.07$ Ry in the whole concentration interval, contrary to the smaller spin-up disorder which changes from $\delta^\uparrow \approx 0.03$ Ry in the Fe-rich alloy to the vanishing value in the Co-rich system.

The same potential parameters can be also used to define local exchange splittings of both components $\Delta_{ex} = C^\uparrow - C^\downarrow$ and their effective Stoner parameters I^{eff} as the ratio of this local splitting to the local magnetic moment. This Stoner parameter is for both elements nearly independent on composition – with relative deviations less then 1 % from the values $I^{eff}_{Fe} = 0.072$ Ry/μ_B and $I^{eff}_{Co} = 0.074$ Ry/μ_B. These values are in agreement with other theoretical results (see Ref. [14], p. 154) and with $I^{eff} \approx 1$ eV/μ_B obtained experimentally for magnetic 3d transition metals [27].

A further interesting question is the charge transfer between the alloy constituents. It has been shown, that the charge transfer from Fe to Co in the ordered FeCo alloy with the CsCl structure is very small, smaller than 0.1 electrons [5]. The charge neutrality is maintained mainly due to the difference in the spin-down atomic levels, the lower position of the Co level leads to higher occupation of the spin-down DOS on the Co atom. Richter and Eschrig [6] performed a study of the disordered bcc $Fe_{100-x}Co_x$ system based on (i) the condition of the local charge neutrality together with (ii) the proportionality of local exchange splittings to local magnetic moments with the effective Stoner parameter $I^{eff} = 0.08$ Ry for both elements. Their results witness, that these two conditions lead to satisfactory compositional dependences of the averaged and local magnetic moments. Our resulting charge transfers were small in the whole composition range, the charge neutrality of each atomic sphere was preserved up to 0.01 electron. This fact justifies both the assumption of local charge neutrality of Refs. [6,7] and our choice of the radii of the atomic spheres.

B. Bulk fcc Ni-Cu

The compositional trend of the Ni magnetic moment in the fcc $Ni_{100-x}Cu_x$ alloys is depicted in Fig. 4. Our values agree reasonably with the results of the KKR-CPA approach [12] as well as with neutron-scattering experiments [10]. The critical Cu concentration for extinction of the Ni moment is approximately 55 at % Cu. The critical concentration was obtained by a linear extrapolation of the squared Ni moment to zero. This extrapolation corresponds to the critical exponent 1/2 common to the mean-field theories [28].

The effective Stoner parameter for Ni obtained from the results in the ferromagnetic region was $I_{Ni}^{eff} = 0.075$ Ry/μ_B and remained constant with a similar accuracy as in the case of I_{Fe}^{eff} and I_{Co}^{eff}. The local moment of Cu atom was negligibly small for all compositions, smaller than 0.01 μ_B. This fact was also found previously from theory [7,11,12,26] and from experiment [10]. However, this negligible Cu moment does not mean that the Cu local DOS is unaffected by the presence of the spin polarized Ni orbitals, as can be seen in Fig. 5 for $Ni_{75}Cu_{25}$. In fact, the tiny Cu moment arises by cancellation of its individual orbital contributions, which are an order of magnitude greater. For example, the total moment of the Cu impurity in Ni, $M_{Cu} = 0.006\ \mu_B$, results from the orbital contributions $M_{Cu}^s = -0.008\ \mu_B$, $M_{Cu}^p = -0.034\ \mu_B$, and $M_{Cu}^d = 0.048\ \mu_B$.

The composition dependence of the Ni moment was theoretically explained on the basis of several mechanisms [7,11], the most important of them being the change in the local Ni DOS and the local charge neutrality, accompanied by an effective charge transfer from the Ni sp states to the Ni d states with increasing Cu content. Our results confirm these findings, as illustrated by Figs. 5-7. The sharp maximum in the DOS occurring for the pure fcc Ni at the top of its d band is strongly reduced in the local Ni DOS for the $Ni_{75}Cu_{25}$ (Fig. 5). This change becomes even more pronounced for the Cu rich alloys, where the Ni DOS can be characterized as a virtual bound state (VBS) below the Fermi level. This indicates a strong level disorder in this alloy system [20] characterized quantitatively by $\delta = (\delta^1 + \delta^\downarrow)/2$, where $\delta^\sigma = C_{Ni}^\sigma - C_{Cu}^\sigma$. The quantity δ takes values between 0.08 Ry for the Ni-rich alloy

and 0.13 Ry for the Cu-rich alloy. The charge transfer between the components was again very small in comparison with the changes in occupations of the up and down Ni-states, see Fig. 6. The largest deviation from the neutrality was found for the Ni impurity in Cu, where about 0.04 electrons were missing in the Ni atomic sphere. The interatomic transfer of Ni electrons from sp to d states is shown in Fig. 7 and amounts to the change of the Ni d filling of 0.13 electrons for the Ni impurity in Cu with respect to pure Ni. Our values of this transfer are about half the published values [11], the reason is probably the perfect chemical short range order of the artificially ordered Ni Cu alloys used in Ref. [11], which enhances this effect.

C. Pure monolayers on Cu(001)

For estimation of the accuracy of our method, the calculated magnetic moments and work functions of pure Fe, Co, and Ni monolayers on the Cu(001) substrate were compared with available results of the full-potential linear augmented plane wave (FLAPW) method [3,9,13] and collected in Table 1. The work function of the clean Cu(001) surface was included as well. One can see a good overall agreement of both approaches, the small differences can have several origins. First, the geometry of the models was not identical. We are using a realistic semiinfinite model of the surface with electronic quantities calculated selfconsistently in five layers, while a single slab with mirror symmetry consisting of seven atomic layers was used in FLAPW calculations. Further, our local moments refer to the slightly overlapping atomic spheres contrary to the muffin-tin spheres in the FLAPW technique. This is probably the reason for our greater local moments, especially for the Fe overlayer, where the d orbitals are less localized than in the Co and Ni cases. The relaxation of the interatomic distances at the surface, which was included for Fe and Co overlayers in Ref. [9] but completely ignored in our study, might also account for several percent reduction of the overlayer moment, similarly as for the Fe bcc(001) surface [3]. The comparison of the work functions reveals systematically larger values obtained with our method, the difference being 0.2 eV for the

surface with overlayers and 0.3 eV for the clean surface. A recent calculation of work functions of elemental metals, performed with a very similar SGF-TB LMTO technique, gave for the Cu(001) surface a value of 5.26 eV [29], in a perfect agreement with our value (Table I). The work function is known to be extremely sensitive to the charge redistribution in the surface region, so that the reasonable agreement between the ASA and full-potential treatments justifies our simple description of the non spherical charge densities via their dipole moments. Having in mind further minor differences between both techniques (e.g. different XC potentials), we can conclude that our SGF-TB-LMTO scheme yields electronic and magnetic quantities comparable to available full potential techniques for chemically perfect overlayers and is therefore well suited for investigations of disordered overlayers.

D. Fe-Co monolayers on Cu(001)

The composition dependences of the local and total magnetic moments in the disordered $Fe_{100-x}Co_x$ overlayers are plotted in Fig. 1. The behavior of the moments is now much simpler than in the bulk: one finds nearly constant magnetic moments of Fe and Co atoms and, consequently, a linear decrease of the total overlayer magnetization with increasing Co content. This picture is quite similar to that found for the Co-rich bulk alloys, the only difference being a slightly greater value of the Fe moment in the overlayer ($\approx 2.9\ \mu_B$) than in the bulk ($\approx 2.6\ \mu_B$). The reason for this similarity is clearly the strong ferromagnetism in both cases, which for the overlayer case extends over the whole composition range, as can be seen from the corresponding overlayer projected DOS's in Fig. 8. Two effects are responsible for this stabilization of the strong ferromagnetism even at the Fe-rich end of the two dimensional alloy: the narrowing of the overlayer DOS due to the reduced number of neighbours at the surface and the pinning of the Fermi energy by the Cu substrate. As a result, the spin up overlayer DOS's are fully occupied at all compositions which leads, together with the local charge conservation in the overlayer discussed below, to the permanent local moments.

Detailed analysis of the local numbers of electrons for both spin orientations is presented in Fig. 3. The conservation of these local numbers is quite pronounced especially in comparison with changes of the Fe-up and Fe-down occupations in the Fe-rich bulk alloys. The local numbers of electrons in the overlayers are generally smaller than those in the bulk (see Fig. 3) which is due to the electronic charge spilt out of the sample. We have found approximately 0.3 electrons in the empty spheres neighbouring to the overlayer. It can be seen from the Fig. 3, that even small changes in the Fe-up and Co-up occupations in the overlayers are compensated by the Fe-down and Co-down occupations, respectively. The total charges in the Fe and Co atomic spheres, amounting respectively to 7.60 and 8.68 electrons, are conserved up to 0.01 electrons throughout the whole composition range. This local charge conservation represents a two-dimensional analogy of the local charge neutrality obtained in the bulk alloys. The local charge conservation at the surface is of the electrostatic origin, its high accuracy reflects the important role of electrostatic interactions for systems with reduced symmetry like the present sample-vacuum interface.

The layer- and component-resolved DOS's for the random $Fe_{50}Co_{50}$ overlayer on the Cu(001) substrate are plotted in Fig. 9 for both spin directions. The spin up local DOS's on Fe and Co atoms are quite similar due to the small level disorder in the overlayer $\delta^1 \approx -0.02$ Ry. This disorder is concentration-independent, has the same small magnitude as in the bulk, and accounts for the rigid-band-like behavior of the overlayer spin up DOS's, see Fig. 8. The spin-down disorder is greater, $\delta^1 \approx 0.01$ Ry, but nearly twice smaller than in the bulk alloy. Nevertheless, this amount of the level disorder together with the present "hopping" disorder are responsible for more pronounced changes in the spin down DOS's on alloying (Fig. 8) as well as for the differences in the component resolved DOS's in the overlayer (Fig. 9). Similarly to the bulk case, the occupation of the spin down Co states is higher than the spin-down Fe states. Contrarily to the bulk case, [illegible] corresponding spin-down levels is located on the Co atoms. The difference in the Fe-down and Co-down occupations contributes significantly to charge balance in the system. The smaller magnitude of δ^1 and the changed sign of δ^1 with respect to the bulk have the same origin.

As can be expected from the less localized wave functions of Fe atoms and seen from the Fig. 3, the electronic deficiency of the Fe atomic spheres in the overlayer is greater than that of the Co spheres. Owing to the intraatomic Coulomb interaction, the Hartree part of the one-electron potentials within the Fe spheres acquires a small negative shift in comparison to the Hartree part of the Co potentials. Assuming that the magnitude of this mutual shift lies between the values of the bulk disorder ($\delta^{\downarrow} \approx 0.015$ Ry, $\delta^{\downarrow} \approx 0.07$ Ry), one can easily understand the reduction of the spin-down disorder with the simultaneous change of sign of the spin-up disorder in the overlayer.

The local DOS's of Fig. 9 can help us to understand the influence of the overlayer on the electronic properties of the Cu substrate layers. A comparison with the bulk Cu DOS shows very small changes in the second subsurface layer while the greater changes in the first subsurface layer are dependent on spin orientation. A stronger perturbation in the spin-down case is due to the larger difference between the substrate (Cu) and overlayer (Fe, Co) atomic d-levels. The local moments of the substrate Cu atoms were very small. In the first subsurface layer, the moments were positive with magnitudes typically 0.013 μ_B, while the second-subsurface moments were negative with smaller magnitudes, typically of 0.008 μ_B.

The effective Stoner parameters for both constituents in the overlayer are now slightly different ($I_{Fe}^{eff} = 0.067$ Ry/μ_B, $I_{Co}^{eff} = 0.071$ Ry/μ_B) from the values in the bulk alloys. Their dependence on the overlayer composition is completely negligible, the relative deviations of I_{Fe}^{eff} and I_{Co}^{eff} were approximately 0.2 % throughout the whole concentration range.

E. Ni-Cu monolayers on Cu(001)

The composition trend of the Ni magnetic moment for the random $Ni_{100-x}Cu_x$ overlayer is shown in Fig. 4. The reduction of the Ni moment in the overlayer with respect to the bulk alloy of the same composition is clearly visible but both dependences are qualitatively very similar. The magnetic moments of Cu atoms were negligible (smaller than 0.01 μ_B)

both in the overlayer and in the substrate layers. The reasons for the smaller Ni moments in the pure Ni overlayer were analyzed in terms of the local DOS [13]. Holes in the Ni-d projected DOS appear even for the spin-up direction (see Fig. 10), contrary to the pure bulk Ni where this DOS is fully occupied. These unoccupied states arise from the Ni-$d_{x^2-y^2}$ orbitals which do not hybridize with other orbitals for symmetry reasons for some $\mathbf{k}_{\parallel}$ point. The Ni/Cu(001) becomes thus a weak ferromagnet with reduced local moment. (Note that similar spin-up holes for the Fe and Co monolayers are eliminated by the greater exchange splitting of these elements.) The effective Stoner parameter for Ni atoms in the random overlayer is $I_{Ni}^{eff} = 0.071$ Ry/μ_B (with 0.5 % tolerance) which is again a slightly smaller value than in the bulk.

The effect of alloying on the overlayer projected DOS's is shown in Fig. 10 for both spin orientations. The DOS's of the pure Ni overlayer and of the clean Cu surface exhibit typical triangle-like shapes due to the band narrowing and an upward shift of potentials at the surface. This upward shift, found as well for clean surfaces [20], has a rather general reason common to metals with more than half-filled bands: the narrowing of the bands at the surface leads to lowering of the local Fermi level below that of bulk bands. To restore its bulk position the surface bands shift upwards. We note that this mechanism is closely related to the so-called surface core-level shifts as the potential changes regards also to the core levels of surface atoms [30]. The DOS's for the intermediate compositions exhibit a pronounced minimum separating the Ni and Cu local DOS's absent in the bulk case [20]. The main reason fort this minimum is the narrowing of the bands at the surface accompanied by an enlarged level disorder in the overlayer case ($\delta = 0.10$ Ry for the pure Ni/Cu(001) overlayer and $\delta = 0.13$ Ry for the Ni-impurity in the Cu(001) surface) compared to the bulk alloy.

The layer- and atom-projected DOS's for the Ni rich overlayer reveal that both elements retain their triangle-shaped narrow local DOS as seen from Fig. 11 for the $Ni_{75}Cu_{25}$ overlayer. This fact is not surprising for the dominating Ni atoms; the same effect for the Cu atoms can be ascribed to the presence of the Cu substrate. Note a negligible spin dependence of all

projected DOS's as a result of the small exchange splitting of Ni. In the Cu-rich overlayers, the local Ni DOS forms the expected VBS below the Fermi energy in complete analogy with the Cu rich bulk case. The only difference here regards the position of these virtual bound Ni levels: the overlayer Ni VBS is located higher than the bulk one.

The numbers of Ni electrons in the overlayer as a function of composition are plotted in the Fig. 6. The spin averaged Ni charge is conserved on alloying roughly to the same accuracy as in the bulk case, while the behavior of the spin-resolved charges follows the trends of the magnetic moments (Fig. 4). The effective charge transfer from Ni-sp states to Ni-d states is substantially reduced in the overlayer, see Fig. 7. The first reason is the fixing of the Fermi energy by the substrate, which causes the increase of the number of Ni-d electrons in the overlayer with respect to the bulk alloy (Fig. 7) despite of the decrease of the total number of Ni electrons by spilling out into the vacuum (Fig. 6). The second reason is the presence of Cu atoms in the first subsurface layer. Similarly as in the bulk alloys [7,11], the internal Ni sp to Ni-d transfer is caused by the Cu alloying and its magnitude is roughly proportional to the number of Cu nearest neighbors of a Ni atom. The change of this Ni-Cu coordination number is three times smaller in the overlayer (4 to 8) than in the bulk (0 to 12) which reduces the internal charge transfer and adds to the first effect.

F. Work functions

The calculated work functions of the random $Fe_{100-x}Co_x$ and $Ni_{100-x}Cu_x$ overlayers are plotted in Fig. 12. The values for pure monolayers on Cu(001) and for a clean Cu(001) surface (Table I) can be reasonably compared to recent values for low-index surfaces of bulk Fe, Co, Ni, and Cu [17,29]. This fact proves that the work function and the electrostatic dipole barrier of a metallic surface are to a great extent controlled by the composition of the topmost layer.

The resulting concentration trends for the random monolayers are nearly linear, a minor continuous change in the slope can be found for the Ni-Cu overlayer (Fig. 12). The linearity

for the $Fe_{100-x}Co_x$ overlayer is not surprising since both components have very similar local electronic properties. In the $Ni_{100-x}Cu_x$ overlayer, no abrupt change of the work function behavior can be seen near the critical concentration $x \approx 45$ at % Cu, where the transition from ferromagnetic to non-magnetic system occurs. This fact is in a qualitative agreement with the smooth behavior observed for the local Ni charge averaged over the spin-up and spin-down parts (Fig. 6). This local Ni charge is completely insensitive to the magnetic phase transition in contrast to the spin-up and spin-down contributions exhibiting a critical behavior with infinite slopes near the transition concentration. In analogy, the smooth behavior of the dipole barrier (and of the work function), which is an electrostatic quantity summed over its two spin contributions, is not striking.

IV. CONCLUSIONS

We have presented a first-principles self-consistent approach to the electronic structure of such complex systems like random ferromagnetic overlayers on noble-metal substrates. The approach is based on the Green's function formalism which makes possible a systematic description of even more complicated systems, e.g. surfaces and interfaces of random alloys with generally inhomogeneous composition profiles and/or with magnetic disorder in the disordered local moment state [31].

We have performed a parallel study of electronic and magnetic properties of random $Fe_{100-x}Co_x$ and $Ni_{100-x}Cu_x$ alloys in the bulk and as monolayers on the Cu(001) substrate. Our results for the bulk alloys compare well with previous studies. For the overlayers, the composition trends of the electronic structure are quite sensitive to the reduced dimensionality of the alloys and to the presence of the substrate and the vacuum. In the Fe-Co overlayers, the strong ferromagnetism is stabilized even at the Fe-rich end, which leads to the enhanced local Fe moments and to the concentration independent local Fe and Co moments. The presence of the Cu substrate supresses the effective Fe $d\downarrow$ to Fe-$d\uparrow$ electron transfer on Co alloying which occurs in the bulk alloys. The presence of the vacuum together with a

different degree of the d-orbital localization of Fe and Co atoms leads to an additional negative shift of Fe potentials, which reduces the strength of the level disorder for the spin-down electrons and changes the sign of the small spin-up disorder with respect to the bulk.

In the Ni-Cu overlayers, the ferromagnetism is weaker than in the bulk alloys of the same composition. The local magnetic moment of Ni is reduced mainly due to the holes in the spin-up Ni-d projected DOS. The critical composition for disappearance of the magnetic order is shifted to the lower Cu concentration as compared to the bulk alloys. The internal charge redistribution from Ni-sp to Ni-d electrons on Cu alloying, which leads to the filling of the Ni-d band in the bulk, is strongly reduced in the overlayer due to the Cu substrate atoms. Their presence is also reflected in the shape of the overlayer-Cu local DOS's even in the Ni-rich overlayers. In the Cu-rich region, the Ni-virtual bound state is shifted to higher energies compared to its bulk position.

In both alloys, two features important for the bulk have their counterparts also in the overlayers. First, it is the effective Stoner behavior relating the local exchange splittings and the local magnetic moments by a simple proportionality. Although the effective Stoner parameters I^{sd} for Fe, Co, and Ni atoms were slightly smaller in the overlayer than in the bulk, they still fall near the value of 1 eV/μ_B found from extensive compilation of experimental results and local density calculations for 3d transition metals in different environments [27]. Second, the local charge neutrality of the individual components in the bulk alloys is modified by the presence of the substrate and the vacuum to the conservation of the local charge of each component in the overlayer. The accuracy of this local charge conservation on changing the overlayer composition is comparable to the bulk case.

Work functions and surface dipole barriers of the random overlayers vary smoothly with their composition. We have found no dramatic change of these quantities near the magnetic phase transition in the Ni-Cu overlayers in accordance with the smooth behavior of the local numbers of Ni electrons summed over both spin orientations.

ACKNOWLEDGEMENTS

The financial support for this work was provided by the Czech Academy of Sciences (Project No. 11015) and the Austrian Science Foundation (P8918).

TABLES

TABLE I. The calculated local magnetic moments M and work functions W for pure Fe, Co, and Ni monolayers on Cu(001) and for clean Cu(001) surface. The values in brackets are results of the slab-FLAPW method, (*a*) - Ref. [9], (*b*) - Ref. [13].

system	M (μ_B)	W (eV)
Fe/Cu(001)	2.80 (2.69[a])	5.29 (5.09[a])
Co/Cu(001)	1.80 (1.79[a])	5.55 (5.34[a])
Ni/Cu(001)	0.41 (0.39[b])	5.67 (5.45[b])
Cu(001)		5.25 (4.94[b])

REFERENCES

[1] L. M. Falicov, D. T. Pierce, S. D. Bader, R. Gronsky, K. B. Hathaway, H. J. Hopster, D. N. Lambeth, S. S. P. Parkin, G. Prinz, M. Salamon, I. K. Schuller, and R. H. Victora, J. Mater. Res. **5**, 1299 (1990).

[2] T. Shinjo, Surf. Sci. Rep. **12**, 49 (1991).

[3] A. J. Freeman and R. Wu, J. Magn. Magn. Mater. **100**, 497 (1991).

[4] D. I. Bardos, J. Appl. Phys. **40**, 1371 (1969).

[5] K. Schwarz, P. Mohn, P. Blaha, and J. Kübler, J. Phys. F **14**, 2659 (1984).

[6] R. Richter and H. Eschrig, J. Phys. F **18**, 1813 (1988).

[7] R. Richter and H. Eschrig, Physica Scripta **37**, 948 (1988).

[8] J. Kaspar and D. R. Salahub, J. Phys. F **13**, 311 (1983).

[9] C. Li, A. J. Freeman, and C. L. Fu, J. Magn. Magn. Mat. **83**, 51 (1990).

[10] R. A. Medina and J. W. Cable, Phys. Rev. **B15**, 1539 (1977).

[11] J. Tersoff and L. P. Falicov, Phys. Rev. **B25**, 4937 (1982).

[12] S. Crampin, R. Monnier, T. Schulthess, G. H. Schadler, and D. D. Vvedensky, Phys. Rev. **B45**, 164 (1992).

[13] D. Wang, A. J. Freeman, and H. Krakauer, Phys. Rev. **B26**, 1340 (1982).

[14] O. K. Andersen, O. Jepsen, and D. Glötzel, in *Highlights of Condensed Matter Theory*, ed. F. Bassani, F. Funi, and M. P. Tosi (North Holland, Amsterdam 1985), p. 59.

[15] J. Kudrnovský and V. Drchal, Phys. Rev. **B41**, 7515 (1990).

[16] J. Kudrnovský, I. Turek, V. Drchal, P. Weinberger, N. E. Christensen, and S. K. Bose, Phys. Rev. **B46**, 1222 (1992).

[17] M. Aldén, S. Mirbt, H. L. Skriver, N. M. Rosengaard, and B. Johansson, Phys. Rev. **B46**, 6303 (1992).

[18] B. Wenzien, J. Kudrnovský, V. Drchal, and M. Šob, J. Phys.: Condens. Matter **1**, 9893 (1989).

[19] H. L. Skriver and N. M. Rosengaard, Phys. Rev. **B43**, 9538 (1991).

[20] J. Kudrnovský, I. Turek, V. Drchal, P. Weinberger, S. K. Bose, and A. Pasturel, Phys. Rev. **B47**, 16525 (1993).

[21] J. Kudrnovský, I. Turek, V. Drchal, and P. Weinberger, Progr. Surf. Sci. (in print).

[22] K. C. Hass, B. Velický, and H. Ehrenreich, Phys. Rev. **B29**, 3697 (1984).

[23] U. von Barth and L. Hedin, J. Phys. C **5**, 1629 (1972).

[24] V. L. Moruzzi, J. F. Janak, and A. R. Williams, *Calculated Electronic Properties of Metals* (Pergamon, New York, 1978).

[25] S. H. Vosko, L. Wilk, and M. Nusair, Can. J. Phys. **58**, 1200 (1980).

[26] S. Blügel, H. Akai, R. Zeller, and P. H. Dederichs, Phys. Rev. **B35**, 3271 (1987).

[27] F. Himpsel, Phys. Rev. Lett. **67**, 2363 (1991).

[28] G. Rickayzen, *Green's Functions and Condensed Matter* (Academic Press, New York, 1980), p. 312.

[29] H. L. Skriver and N. M. Rosengaard, Phys. Rev. **B46**, 7157 (1992).

[30] M. Methfessel, D. Hennig, and M. Scheffler, Phys. Rev. **B46**, 4816 (1992).

[31] B. L. Gyorffy, A. J. Pindor, J. Staunton, G. M. Stocks, and H. Winter, J. Phys. F **15**, 1337 (1985).

FIGURES

FIG. 1. The average and local magnetic moments in the random bulk bcc $Fe_{100-x}Co_x$ alloys (open symbols) and in the random $Fe_{100-x}Co_x$ overlayers on the Cu(001) substrate (full symbols) as a function of composition.

FIG. 2. Densities of states for the random bcc $Fe_{50}Co_{50}$ alloy for both spin directions: average DOS (full), Fe local DOS (dashed), and Co local DOS (dotted). The vertical lines denote the Fermi level.

FIG. 3. Concentration dependence of component- and spin-resolved numbers of electrons in the random bcc $Fe_{100-x}Co_x$ alloys (open squares) and in the random $Fe_{100-x}Co_x$ overlayers on the Cu(001) substrate (full squares): (a) Fe-up electrons, (b) Fe-down electrons, (c) Co-up electrons, and (d) Co-down electrons.

FIG. 4. The local magnetic moments of Ni atoms in the random bulk fcc $Ni_{100-x}Cu_x$ alloys (open squares) and in the random $Ni_{100-x}Cu_x$ overlayers on the Cu(001) substrate (full squares) as a function of composition. The extrapolation to the non-magnetic state is marked in dashes (see text for details).

FIG. 5. Densities of states for the random fcc $Ni_{75}Cu_{25}$ alloy for both spin directions: average DOS (full), Ni local DOS (dashed), and Cu local DOS (dotted). The vertical lines denote the Fermi level.

FIG. 6. Concentration dependence of spin-up (triangles), spin-down (circles), and spin-averaged (squares) numbers of Ni electrons in the random fcc $Ni_{100-x}Cu_x$ alloys (open symbols) and in the random $Ni_{100-x}Cu_x$ overlayers on the Cu(001) substrate (full symbols). The extrapolation to the non-magnetic state is marked in dashes (see text for details).

FIG. 7. Concentration dependence of the numbers of Ni-sp and Ni-d electrons in the random fcc $Ni_{100-x}Cu_x$ alloys (open symbols) and in the random $Ni_{100-x}Cu_x$ overlayers on the Cu(001) substrate (full symbols).

FIG. 8. Spin-resolved overlayer densities of states for the random $Fe_{100-x}Co_x$ overlayers on the Cu(001) substrate as a function of composition: (a) up-spin orientation and (b) down-spin orientation. The vertical lines denote the substrate Fermi level.

FIG. 9. Layer- and component-resolved densities of states in the random $Fe_{50}Co_{50}$ overlayer on the Cu(001) substrate: (a) up-spin orientation and (b) down spin orientation. The overlayer (ov) component DOS's (Fe - full, Co - dashed) and the first (s1) and second (s2) substrate layer DOS's are given. The bulk Cu DOS is also included. The vertical lines denote the substrate Fermi level.

FIG. 10. Spin-resolved overlayer densities of states for the random $Ni_{100-x}Cu_x$ overlayers on the Cu(001) substrate as a function of composition: (a) up-spin orientation and (b) down-spin orientation. The vertical lines denote the substrate Fermi level.

FIG. 11. Layer- and component-resolved densities of states in the random $Ni_{75}Cu_{25}$ overlayer on the Cu(001) substrate: (a) up-spin orientation and (b) down-spin orientation. The overlayer (ov) component DOS's (Ni - full, Cu - dashed) and the first (s1) and second (s2) substrate layer DOS's are given. The bulk Cu DOS is also included. The vertical lines denote the substrate Fermi level.

FIG. 12. The work functions of the random $Fe_{100-x}Co_x$ and $Ni_{100-x}Cu_x$ overlayers on the Cu(001) substrate as a function of composition.

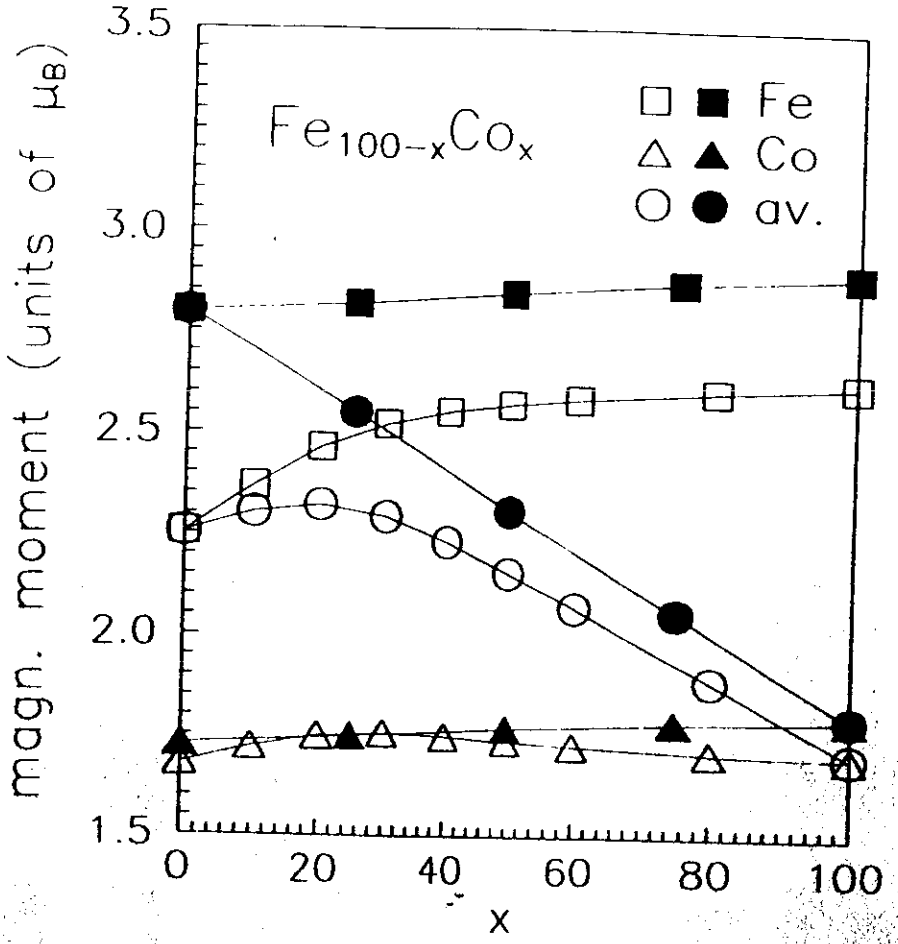
3.5
3.0
2.5
2.0
1.5
magn. moment (units of μ_B)
$Fe_{100-x}Co_x$
Fe
Co
av.
0
20
40
60
80
100
x

Fig. 1

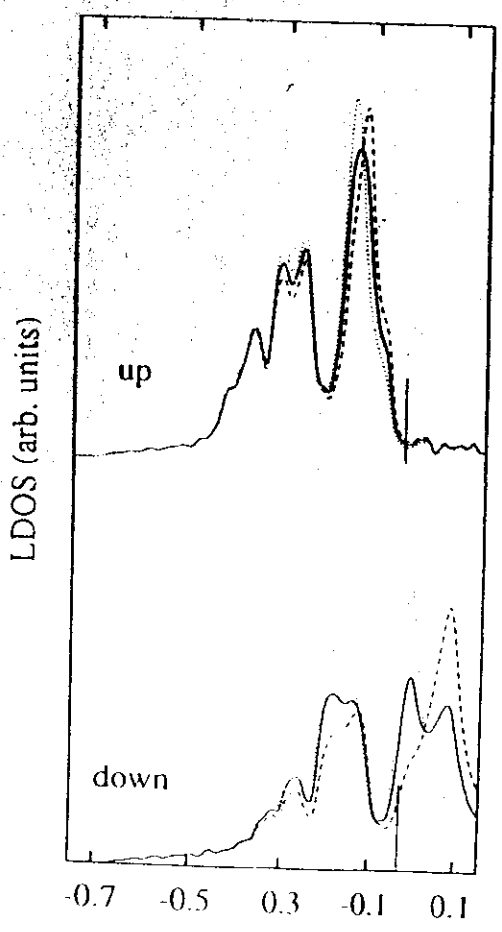
LDOS (arb. units)
up
down
-0.7
-0.5
0.3
-0.1
0.1

Fig. 2

Figs. 3(a-d)

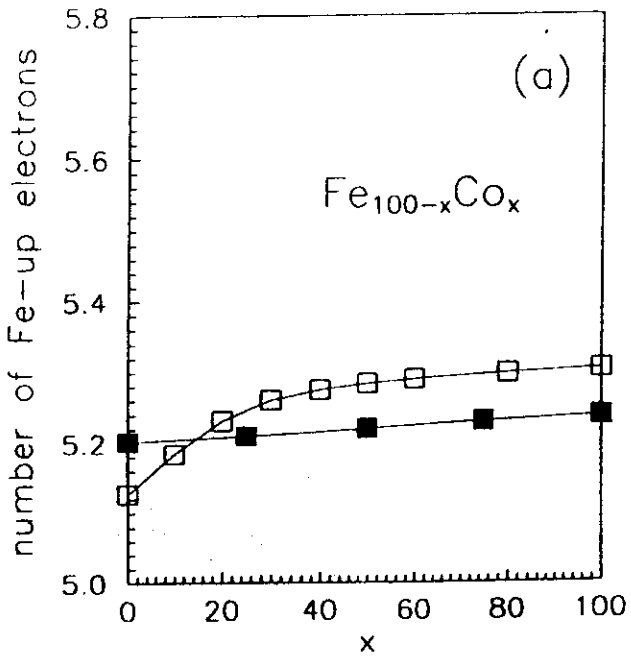
(a)
$Fe_{100-x}Co_x$
number of Fe-up electrons
5.8
5.6
5.4
5.2
5.0
0
20
40
60
80
100
x

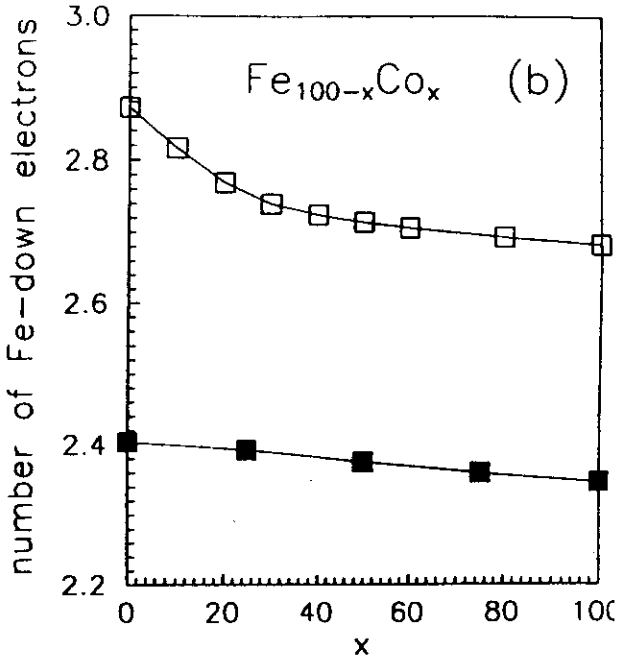
(b)
$Fe_{100-x}Co_x$
number of Fe-down electrons
3.0
2.8
2.6
2.4
2.2
0
20
40
60
80
x

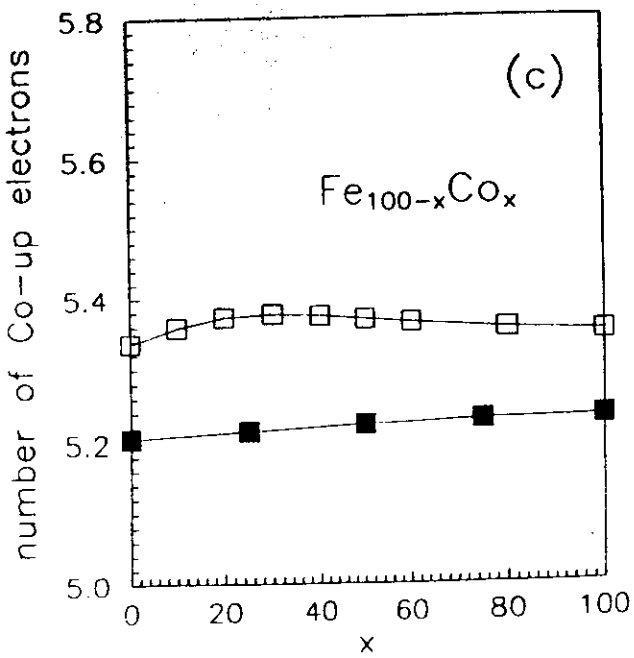
(c)
$Fe_{100-x}Co_x$
number of Co-up electrons
5.8
5.6
5.4
5.2
5.0
0
20
40
60
80
100
x

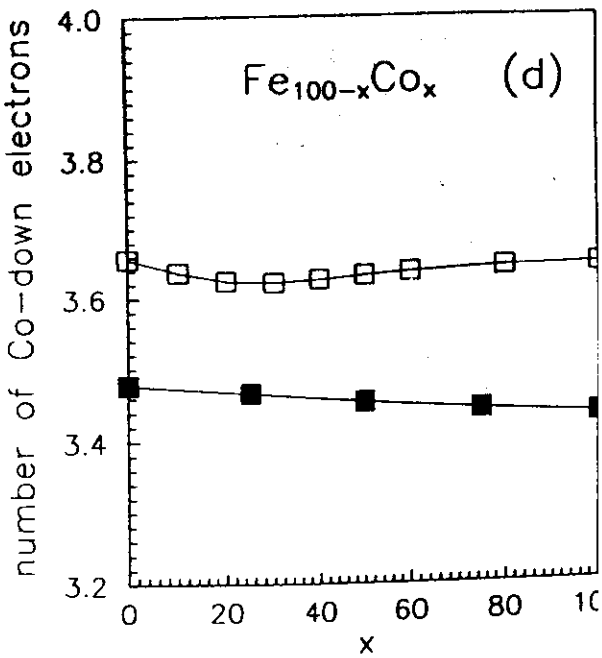
(d)
$Fe_{100-x}Co_x$
number of Co-down electrons
4.0
3.8
3.6
3.4
3.2
0
20
40
60
80
x

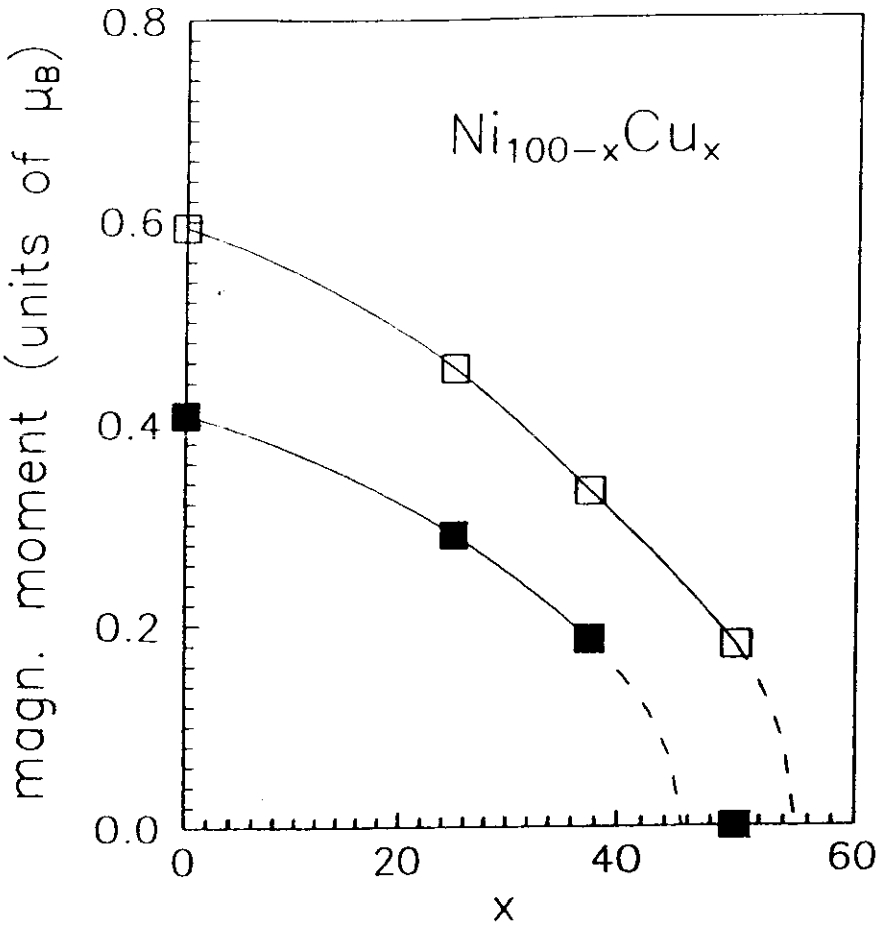
0.8
0.6
0.4
0.2
0.0
magn. moment (units of μ_B)
$Ni_{100-x}Cu_x$
0
20
40
60
x

Fig. 4

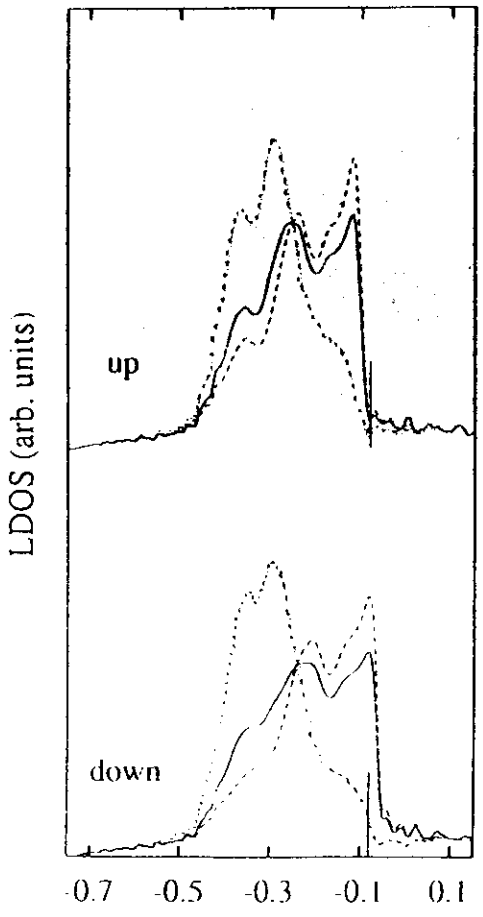
LDOS (arb. units)
up
down
-0.7
-0.5
-0.3
-0.1
0.1

Fig. 5

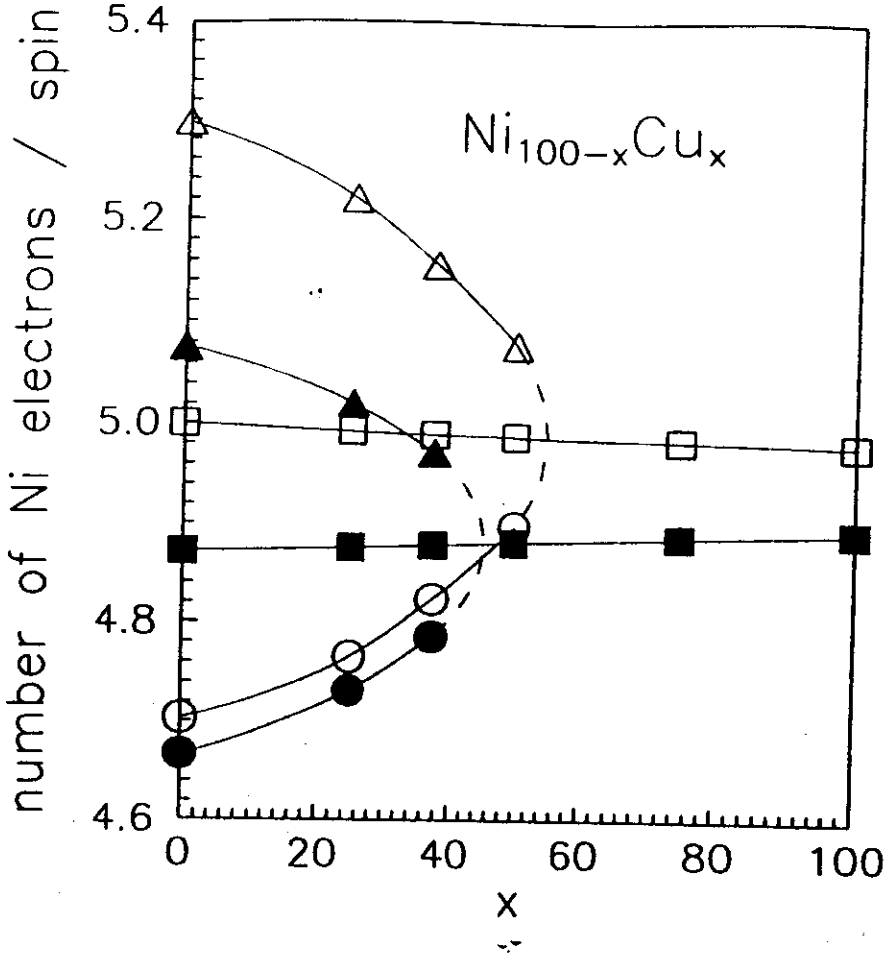
number of Ni electrons / spin
5.4
5.2
5.0
4.8
4.6
$Ni_{100-x}Cu_x$
0
20
40
60
80
100
x

Fig. 6

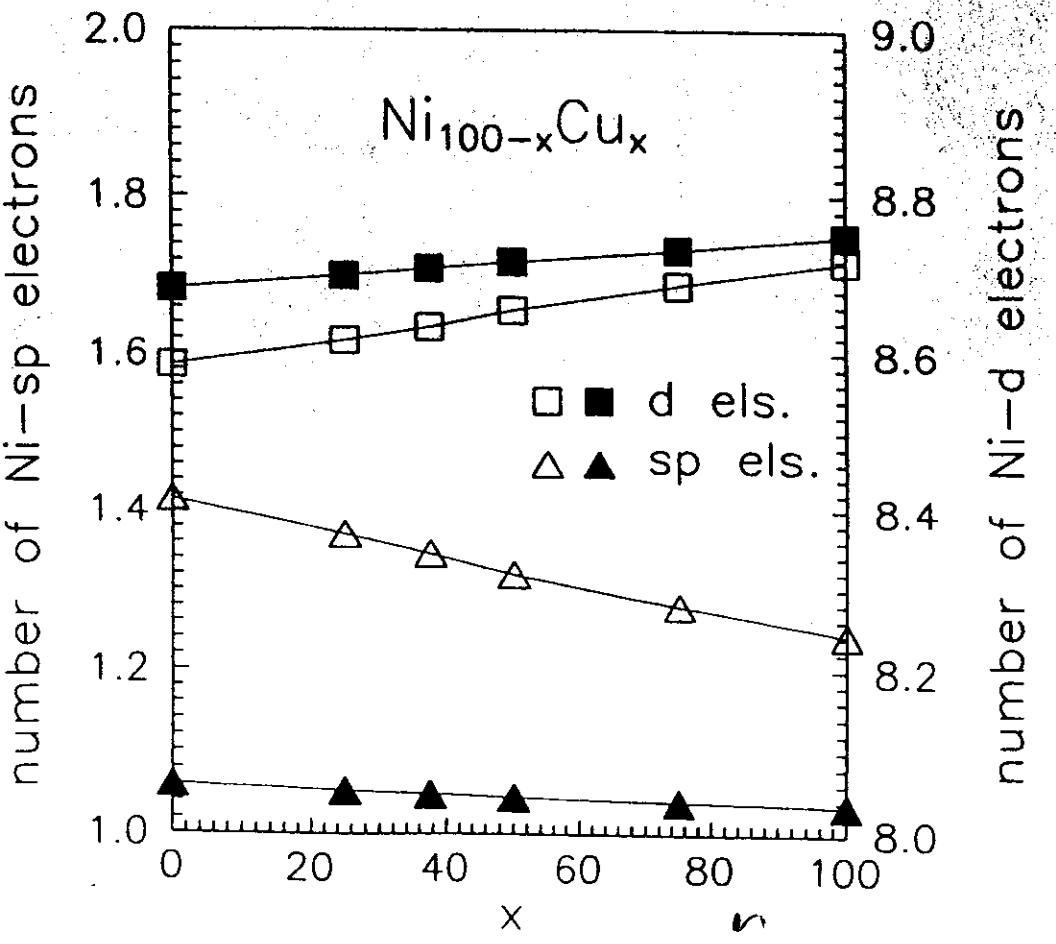
number of Ni-sp electrons
number of Ni-d electrons
2.0
1.8
1.6
1.4
1.2
1.0
9.0
8.8
8.6
8.4
8.2
8.0
$Ni_{100-x}Cu_x$
d els.
sp els.
0
20
40
60
80
100
x

Fig. 7

Fig. 8

(a)

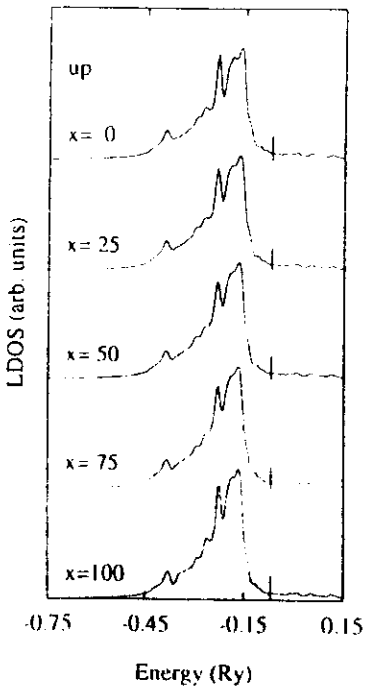

(b)

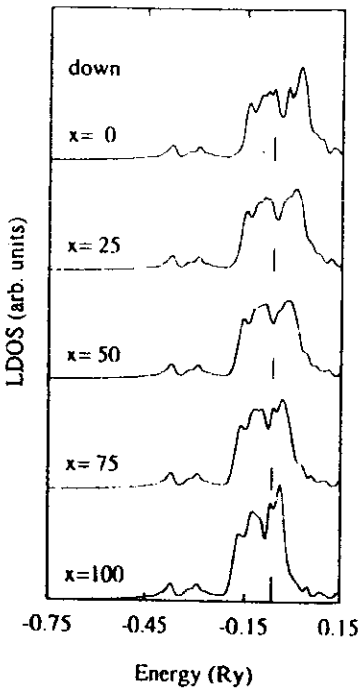

Fig. 9

(a)

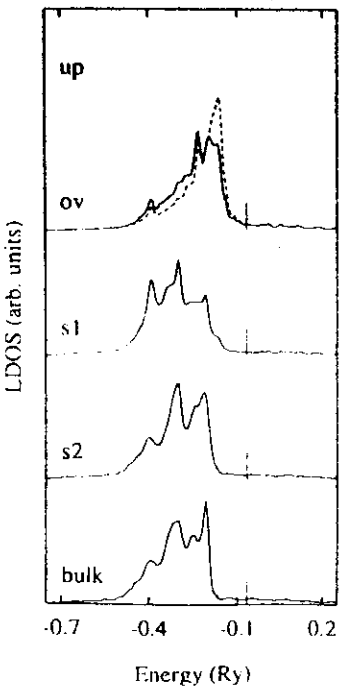

(b)

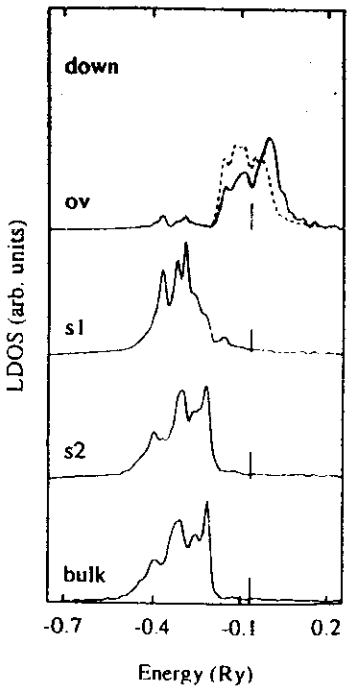

Fig. 10

(a)

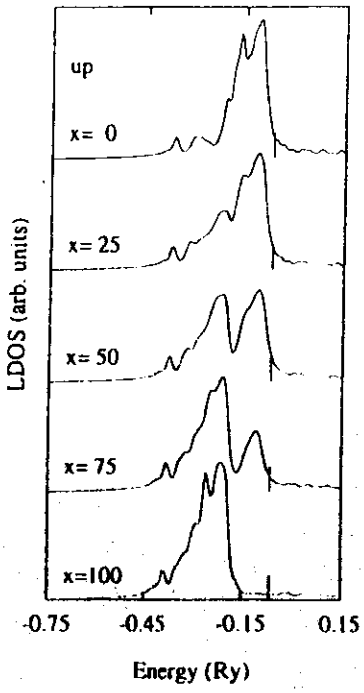

(b)

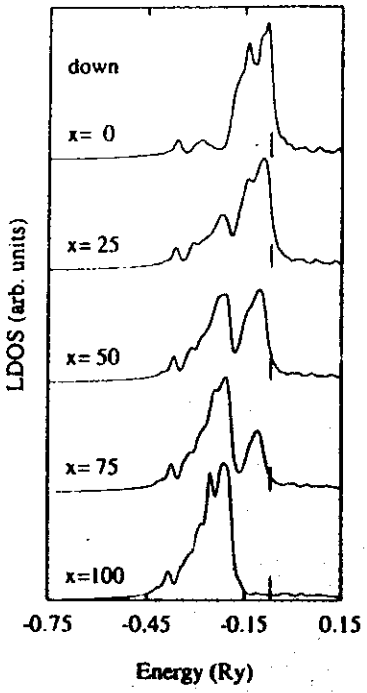

Fig. 11

(a)

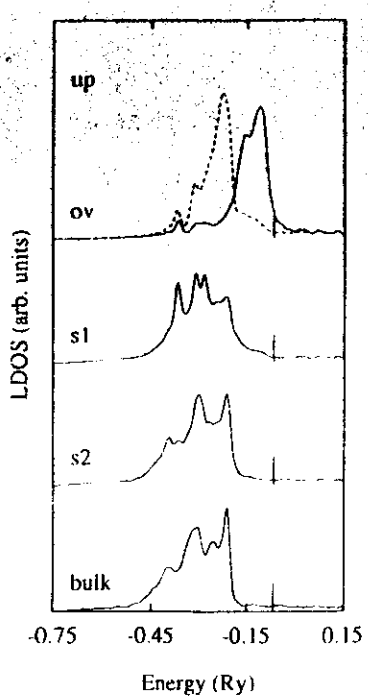

(b)

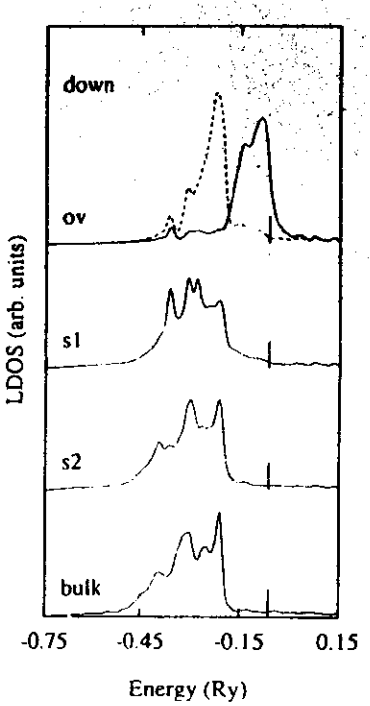

Fig. 12

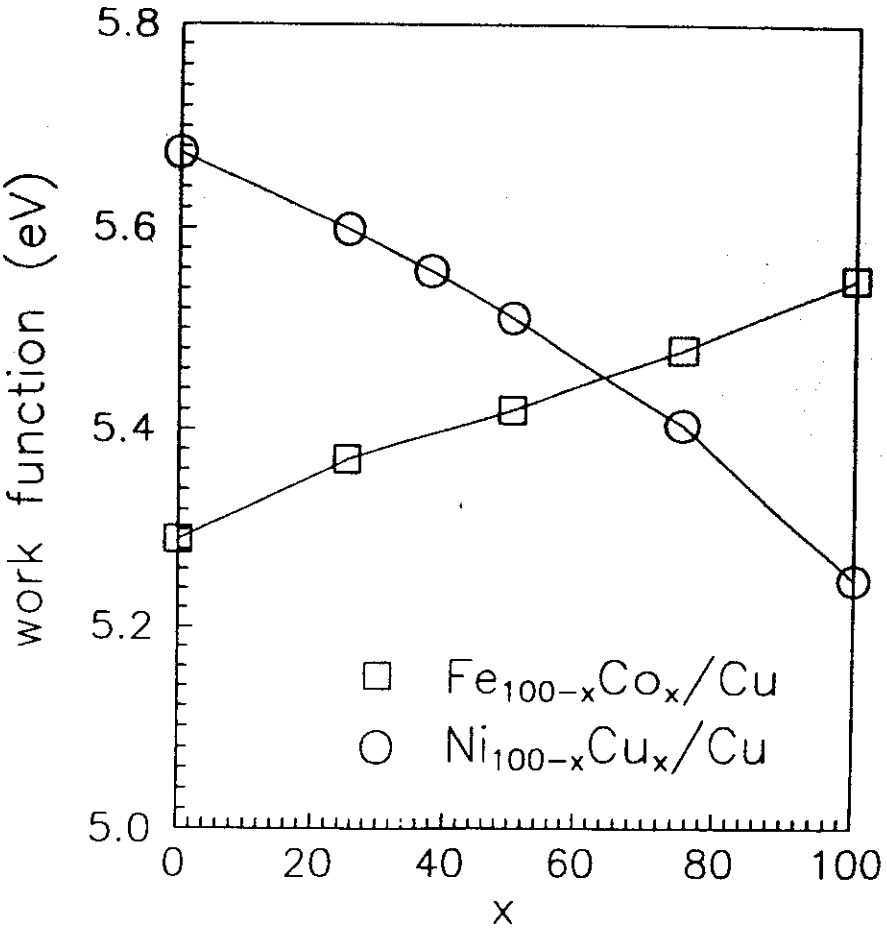
5.8
5.6
5.4
5.2
5.0
work function (eV)
0
20
40
60
80
100
x
Fe100-xCox/Cu
Ni100-xCux/Cu